ATOMIC FORCE MICROSCOPY USING A PIEZORESISTIVE CANTILEVER

M. Tortonese, H. Yamada* , R. C. Barrett, and C. F. Quate

E. Ginzton Laboratory, Stanford University, Stanford, CA 94305 U.S.A.

Abstract: An atomic force microscope (AFM) is an instrument which measures the topography of a surface by bringing a cantilever beam into contact with a sample and measuring the deflection of the cantilever as it is scanned across the surface. The complexity of an AFM is predominantly governed by the detector used for measuring the deflection of the cantilever probe. In this paper we describe the fabrication of a silicon cantilever beam with an integrated piezoresistor for sensing its deflection. A silicon on insulator (SOI) material is used for the fabrication. A p-type resistor is fabricated at the surface of the cantilever along a <110> direction so that the piezoresistive effect of silicon causes its resistance to vary linearly with its deflection. Our cantilevers typically have spring constants from 1 to 10 N/m and minimum detectable deflections (MDD) from 1 to 10 Å over a 10 Hz - 1 KHz frequency range. We successfully used the cantilevers in an AFM and present an image of a grating obtained with this technique.

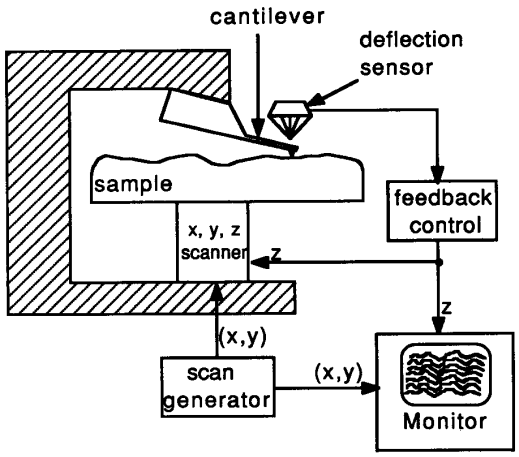

Fig. 1: Block diagram of an AFM

Introduction

The AFM [1] is schematically illustrated in Fig. 1. In the contact repulsive operation mode, which is one of the most common for AFM, a cantilever beam is brought into contact with a sample. The sample is scanned and the cantilever deflects according to the topography of the sample. The sensor measures the deflection of the cantilever and, through a feedback loop, adjusts the z translator of the sample to keep the deflection of the cantilever constant. The applied vertical displacement of the sample is used as the imaging signal. The problem of measuring the deflection of the cantilever beam is crucial in AFM. All the present methods use some external physical component which is brought close to the cantilever. The most commonly used technique is to focus a laser beam onto the cantilever and to measure the deflection of the reflected beam with a photodetector [2]. Though very sensitive to cantilever deflections, this technique requires the use of precisely aligned optical components. This introduces complications in the design and operation of an AFM. One limitation is that it is difficult to scan the cantilever because of the complexity of the deflection sensor associated with it. The cantilevers used in AFM are usually made with silicon micromachining techniques [3]. Microfabricated cantilevers offer excellent characteristics in terms of small spring constants and high resonant frequencies. Furthermore, sharp tips can be integrally fabricated on them [4] and batch fabrication processes yield cantilevers with very reproducible characteristics. Microfabricated cantilever beams with integrated piezoelectric [5] and capacitive [6] actuators have previously been built for use in AFM and related fields. We chose to explore the piezoresistive effect since it has been successfully used to measure cantilever deflections in other applications [7]. In this paper we describe a cantilever beam with an integrated piezoresistive deflection sensor for use in an AFM. This cantilever requires no external deflection-sensing components, simplifying the AFM design for new applications. In particular, since the cantilever can be scanned, the AFM may prove useful in profilometry and integrated circuit inspection. Also, operations in vacuum and at low temperature would considerably benefit from the lack of external deflection sensing components.

Device Fabrication

The device cross section and plan view are illustrated in Fig. 2. The fabrication sequence requires four lithographies. The starting material is a silicon on insulator (SOI) wafer manufactured using wafer-bonding technology [8]. The intermediate oxide layer is used as an etch stop during the process of etching the bulk silicon substrate in one of the last fabrication steps. The top layer is n-type silicon, 15 Ω cm, 6 ± 1 μm thick, and the intermediate oxide layer is 1 μm thick (Fig. 2a). The first step in the process is to etch the top

* present address: Quantum Metrology Department, National Research Laboratory of Metrology, 1-1-4 Umezono Tsukuba 305 Japan

91CH2817-5/91/0000-0448$01.00 © 1991IEEE

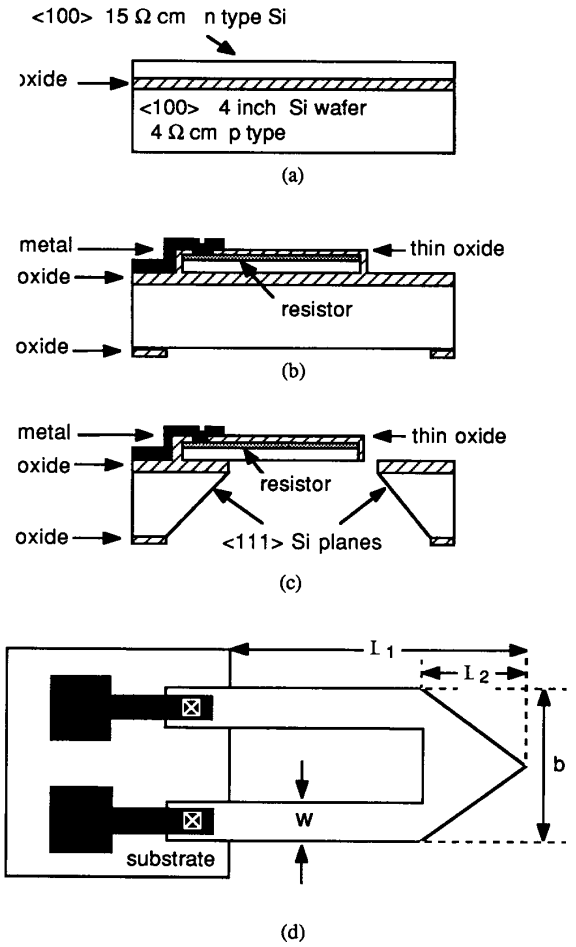

Fig. 2: Fabrication process. (a) starting material. (b) cross-section before final etch. (c) cross-section of the final device. (d) plan view of the final device

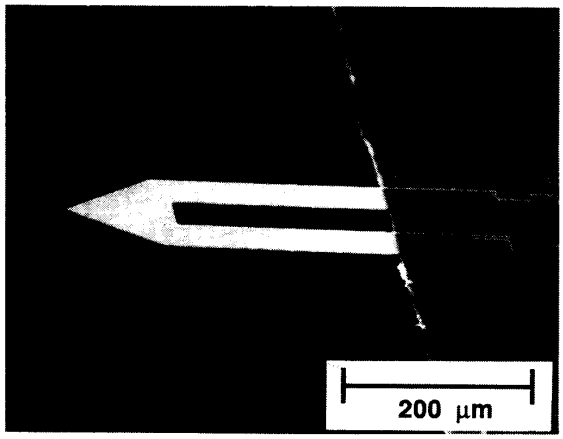

Fig. 3: SEM micrograph of a cantilever.

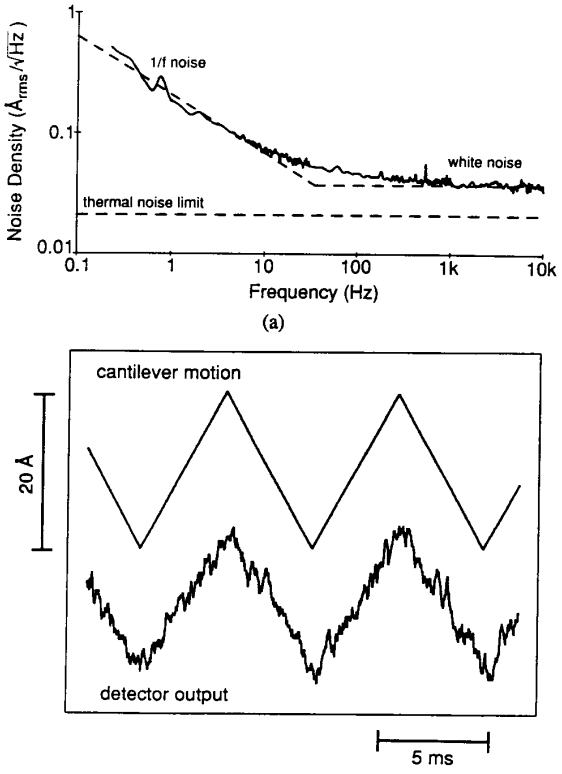

Fig. 4: noise characteristics of the piezoresistive cantilever with the bridge biased with ±5 V. (a) noise spectrum. (b) response to 20 Å cantilever motion

silicon layer down to a thickness of 2 ± 1 µm. Then the wafer is oxidized. The frontside oxide is etched and boron is implanted at 80 keV, 10^{15} ions/cm^2. The resulting sheet resistance for the piezoresistors is 150 Ω/sq. At this point both the frontside and backside are patterned: on the backside large windows are opened, through which the bulk silicon will be etched in one of the last steps of the process; on the frontside the cantilevers are patterned. The cantilevers are formed by etching the frontside silicon until the intermediate oxide layer stops the etch. A thin oxide is then grown as a passivating layer on the surface of the cantilever. Contact holes are opened and aluminum is sputtered, patterned and etched to provide contacts to the resistors (Fig. 2b). After annealing the contacts, a polyimide layer is spun on the frontside of the wafer and the bulk silicon is etched from the backside in ethylene diamine, pyrocathecol, and water (EDP). The polyimide layer, fully imidized, protects the frontside from the EDP solution. At the end of this etch the original SOI oxide layer is etched and the polyimide is removed so that the cantilever is released and the final structure is obtained (Fig. 2c). Fig. 2d shows a plan view drawing of a cantilever. Fig. 3 is a scanning electron microscope micrograph of a

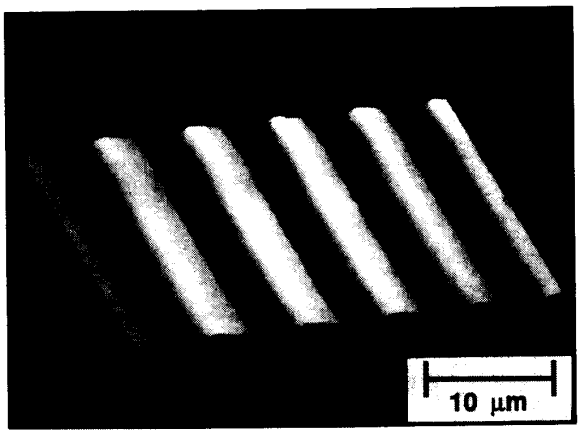

Fig. 5: Image of a silicon dioxide grating taken with a piezoresistive cantilever. The period is 6.5 µm and the height is 270 Å.

completed cantilever. The metal contacts are visible on the right side of the picture.

Results

Several cantilevers with different sizes have been fabricated and used for imaging in an AFM. The results reported here were generated using a cantilever with the following specifications: R=2.5 kΩ, L_1=175 µm, L_2=75 µm, w=20 µm, b=90 µm, t=2 µm. Its calculated spring constant is 4 N/m. The measured sensitivity of the cantilever in terms of ΔR/R is $1.2\text{x}10^{-7}$ $Å^{-1}$. Fig. 4 shows the noise characteristics of the cantilever. Fig. 4a shows the noise spectrum recorded with the cantilever free-standing in air. For this measurement the bridge was biased with ±5 V. The integrated noise from 0.01 Hz to 1 KHz is equivalent to 1.35 $Å_{rms}$. This is the minimum detectable deflection (MDD) over the given frequency range for a signal-to-noise ratio of 1. The corner frequency of the 1/f noise is 35 Hz. The excess white noise above the thermal noise limit is due to the amplifier. Fig. 4b shows the response of the piezoresistor to a cantilever motion of 20 Å. This plot was obtained by bringing the cantilever into contact with a sample and by moving the sample with a piezoelectric actuator. Fig. 5 shows an image of a silicon dioxide grating taken with this cantilever. The grating has a period of 6.5 µm and a depth of 270 Å.

Device Analysis and Characterization

Two important parameters for describing this device for imaging are its spring constant and MDD. The spring constant should be low so that the cantilever does not exert too much force on the sample and damage it. The MDD determines the vertical resolution of the microscope and should therefore be minimized. Other important characteristics such as a high resonant frequency and robustness are largely automatically met by microfabricated silicon cantilevers. For the cantilever geometry shown in Fig. 2d, the spring constant can be calculated to be:

$$K = \frac{E\, t^3\, w\, b}{(L_1^3 - L_2^3)\, b + 3\, L_2^3\, w} \qquad (1)$$

where E is the Young's modulus of silicon, t is the thickness of the cantilever and w, b, L_1 and L_2 are defined in Fig. 2d.

When the cantilever is deflected the piezoresistor changes its resistance. In order to calculate the change in resistance we make two simplifying assumptions: first, we assume that the triangular portion of the cantilever does not contribute to the cantilever resistance. This assumption is valid because the wide triangular region has a much smaller resistance than the narrow legs. Second, we neglect the thickness of the passivating thin oxide layer and assume that the current in the resistor flows at the surface of the cantilever. This assumption is certainly not adequate for our device because the thermal cycles following the ion implantation drive the doping profile toward the middle plane of the cantilever and this reduces the expected change in resistance. Under the stated assumptions, the relative change in resistance for a given force applied to the free end of the cantilever is:

$$\frac{\Delta R}{R} = \pi_l S = \frac{3\, \pi_l\, (L_1 + L_2)}{4\, w\, t^2} F \qquad (2)$$

where π_l is the longitudinal piezoresistive coefficient of silicon for the <110> direction, at the operating temperature and at the given doping concentration of the resistor, S is the effective longitudinal stress in the resistor and F is the applied force. It is useful for our application to write the relative resistance change in terms of the displacement of the free end of the cantilever because that displacement is directly related to the topography of the sample:

$$\frac{\Delta R}{R} = \frac{3\, \pi_l\, E\, t\, b\, (L_1 + L_2)}{4\, [(L_1^3 - L_2^3)\, b + 3\, L_2^3\, w]} z \qquad (3)$$

where z is the displacement of the free end of the cantilever.

The minimum detectable signal is determined by the noise level in the measurement of the resistance. This is ultimately limited by the thermal noise in the bridge resistors. Assuming the bridge is made up of four resistors of resistance R, the minimum detectable resistance change is given by:

$$\left(\frac{\Delta R}{R}\right)_{min} = \frac{2\sqrt{4\, k\, T\, R\, \Delta f}}{V} = 4\sqrt{\frac{k\, T\, \Delta f}{P}} \qquad (4)$$

where k is the Boltzmann constant, T is the absolute temperature, Δf is the bandwidth, P is the power dissipated in the piezoresistor and

the bridge is biased with ±V. The MDD (z_{min}) and the minimum detectable force (F_{min}) can finally be calculated as:

$$z_{min} = \frac{4\,[(L_1^3 - L_2^3)\,b + 3\,L_2^3\,w]}{3\,\pi_l\,E\,t\,b\,(L_1 + L_2)} \left(\frac{\Delta R}{R}\right)_{min} \xrightarrow{L_1 >> L_2} \frac{3L_1^2}{4\pi_l\,E\,t} \left(\frac{\Delta R}{R}\right)_{min} \quad (5)$$

and

$$F_{min} = \frac{4\,w\,t^2}{\pi_l\,(L_1 + L_2)} \left(\frac{\Delta R}{R}\right)_{min} \quad (6)$$

On the basis of this analysis we can make some simple but useful considerations on how to optimize the design for our specific application. From an electrical point of view, the MDD does not depend upon the resistance of the piezoresistor for a fixed maximum allowable power dissipation in the resistor. From a mechanical point of view, the ideal characteristics for a cantilever for use in an AFM are a low spring constant (near 1 N/m) and a MDD as small as possible. From equations (1) and (5) it is evident that it is advantageous to make w as small as possible. Therefore w can be chosen to be the smallest value that can be fabricated and that guarantees enough lateral stiffness for the cantilever. The length and the thickness of the cantilever also should be made small. By scaling down the length and the thickness proportionally, the spring constant is held constant, while the minimum detectable deflection is reduced. The minimum thickness is ultimately determined by the doping profile of the resistor. If the current flow in the resistor approaches the middle plane of the cantilever, then the sensitivity drops dramatically. In our process we fixed the thickness of the cantilever at 2 μm. Therefore the only free parameter left is the length of the cantilever. Long cantilevers will have smaller spring constant and less sensitivity than short cantilevers. Long cantilevers may therefore be used to image soft samples when high vertical resolution is not required and short cantilevers may be used to image hard samples with high vertical resolution.

Conclusions

In this paper we have presented a new microfabricated piezoresistive cantilever for use in AFM. We outlined one possible way of characterizing and optimizing the cantilever design in view of its application in AFM. We have built and characterized a piezoresistive cantilever and we demonstrated its use by imaging a 6.5 μm pitch, 270 Å deep, silicon dioxide grating. Table 1 summarizes the characteristics of the cantilever used to take the image.

Future improvements concern the fabrication of an integral tip at the free end of the cantilever so that higher lateral resolution can be obtained, and the fabrication of shallower resistors so that the MDD of the cantilever can be reduced.

Given the simplification in the microscope design made possible through the use of this cantilever the AFM can become more useful for applications such as profilometry, metrology and integrated circuit inspection. Applications in adverse environments such as ultra-high vacuum and low temperature also become simpler. In particular, operation of the cantilever at low temperature (above the temperature at which carriers freeze-out) should improve the cantilever performance because of reduced Johnson noise and increased piezoresistance coefficient.

Table 1: characteristics of one of the fabricated cantilevers

Dimensions:	L_1 = 175 μm, L_2 = 75 μm, w = 20 μm, b = 90 μm, t = 2 μm
Resistance:	2.5 kΩ
Spring constant (calculated):	4 N/m
Sensitivity (ΔR/R):	1.2×10^{-7} Å^{-1}
Minimum detectable deflection: (bias = ±5 V, 0.01Hz-1KHz)	1.35 $Å_{rms}$
Minimum detectable force: (bias = ±5 V, 0.01Hz-1KHz)	5.4×10^{-10} N_{rms}

We acknowledge Shin Etsu Japan for providing the SOI wafers, Shinya Akamine, Kan Nakayama and Jun Nogami for useful discussions. This work was supported by the National Science Foundation and the Joint Services Electronics Program. One of the authors (RCB) acknowledges the support of the Fannie and John Hertz Foundation.

References

[1] G. Binnig, C. F. Quate, and Ch. Gerber, Phys. Rev. Lett. **56**, 1164 (1986).

[2] G. Meyer and N. M. Amer, Appl. Phys. Lett. **53**,1045 (1988).

[3] T. R. Albrecht, S. Akamine, T. E. Carver, and C. F. Quate, J. Vac. Sci. Technol. A **8**, 3386 (1990).

[4] S. Akamine, R. C. Barrett, and C. F. Quate, Appl. Phys. Lett. **57**, 316 (1990).

[5] S. Akamine, T. R. Albrecht, M. J. Zdeblick, and C. F. Quate, IEEE Electron Dev. Lett. **10**, 490 (1989).

[6] L. C. Kong, B. G. Orr, and K. D. Wise, J. Vac. Sci. Technol., in press.

[7] L. M. Roylance, and J. B. Angell, IEEE Trans. Electron Dev. **ED-26**, 1911 (1979).

[8] T. Abe, M. Nakano, and T. Itoh, Proc. 4th Int. Symp. on Silicon-on-Insulator Technology and Devices, May 6-11, 1990, Montreal.